Supporting Information for

Constructing stable charge redistribution through strong metal-support interaction for overall water splitting in acidic solution

Yanyun Zhang,[a,‡] Hao Huang,[d,‡] Yi Han,[a] Yingnan Qin,[a] Nanzhu Nie,[a,b] Wenwen Cai,[a] Xinyi Zhang,[a] Zhenjiang Li,[c] Jianping Lai [a,*] and Lei Wang[a,b,*]

[a]Key Laboratory of Eco-chemical Engineering, Ministry of Education, Taishan scholar advantage and characteristic disci-pline team of Ecochemical progress and technology, Laboratory of Inorganic Synthesis and Applied Chemistry, College of Chemistry and Molecular Engineering, Qingdao University of Science and Technology, Qingdao 266042, P. R. China

[b]Shandong Engineering Research Center for Marine Environment Corrosion and Safety Protection, College of Environment and Safety Engineering, Qingdao University of Science and Technology, Qingdao 266042, P. R. China

[c]College of Materials Science and Engineering, Qingdao University of Science and Technology, Qingdao 266061, Shandong, PR China

[d]Department of Microsystems, University of South-Eastern Norway, Borre 3184, Norway

‡Equal contribution.

Experimental Section

Chemicals. Platinum (II) acetylacetonate (97%), Ruthenium (III) acetylacetonate (97%) and perchloric acid ($HClO_4$, 70%) were all bought from Sigma-Aldrich. Ketjen black (KB, Carbon EC600JD) was bought from Aladdin. The solutions were freshly prepared with deionized water (18.2 MΩ/cm).

Preparation of Pt-RuO_2@KB. Firstly, 9 mg of processed. Ketjen black (KB, Carbon EC600JD), 6 mg Ruthenium (III) acetylacetonate and 3 mg Platinum (II) acetylacetonate were mixed and ground in a mortar for 30 minutes to mix evenly. Then, the mixture was put into a 10 mL quartz bottle and microwaved in a

household microwave oven for 5 minutes. The reaction mixture was then washed with 30 mL of Ethanol to obtain a black powder.

Preparation of RuO_2@KB. Firstly, 9 mg of processed. Ketjen black (KB, Carbon EC600JD) and 6 mg Ruthenium (III) acetylacetonate were mixed and ground in a mortar for 30 minutes to mix evenly. Then, the mixture was put into a 10 mL quartz bottle and microwaved in a household microwave oven for 5 minutes. The reaction mixture was then washed with 30 mL of Ethanol to obtain a black powder.

Preparation of Pt@KB. Firstly, 9 mg of processed. Ketjen black (KB, Carbon EC600JD) and 6 mg Platinum (II) acetylacetonate were mixed and ground in a mortar for 30 minutes to mix evenly. Then, the mixture was put into a 10 mL quartz bottle and microwaved in a household microwave oven for 5 minutes. The reaction mixture was then washed with 30 mL of Ethanol to obtain a black powder.

Characterization. The morphologies of as-prepared catalysts were conducted by transmission electron microscope (TEM, HITACHI HT7800) at 100 kV and scanning electron microscope (SEM, HITACHI regulus8100) at 15 kV. The high-resolution transmission microscopy (HRTEM) images and energy dispersive X-ray spectroscopy (EDS) were taken by JEOL JEM-F200. Powder X-ray diffraction (XRD) spectra were recorded on an X'Pert-Pro X-ray powder diffractometer equipped with a Cu radiation source (λ = 0.15406 nm). The chemical valence of each element was collected by X-ray photoelectron spectra (XPS) on SSI SProbe XPS Spectrometer. The composition of as-prepared samples was collected by the inductively coupled plasma-atomic emission spectroscopy (ICP-AES, Agilent 8800). The catalyst that has been tested for stability is scraped from the working electrode by ultrasonic treatment and collected for the next step of TEM and XRD characterization.

Electrochemical measurements. Before the electrochemical tests, the as-prepared catalysts were dispersed in a mixture of ultrapure water, isopropanol and 5 wt% Nafion solution (v: v: v = 1: 1: 0.01) and then sonicated for 1 h to obtain homogeneous catalyst ink with concentration of 1 mg mL^{-1}. Subsequently, 10 μL of the catalyst ink was dropped onto the surface of the GCE for further electrochemical tests. All the electrochemical tests were conducted by CHI660E electrochemical workstation (Chenhua, Shanghai) with a traditional three-electrode system. The catalysts modified glass carbon electrode (GCE) was used as working electrode, a Pt foil was used as counter electrode, and a saturated calomel electrode (SCE) was used as reference electrode. The potential was calibrated by the Nernst equation that $E_{RHE} = E_{SCE} + 0.242 + 0.0592$ pH. Before each test, GCE was polished by Al_2O_3 powder to get a smooth surface. And take 10μL of the mixed slurry and drop it evenly on the surface of the GCE, after it is naturally dried, further electrochemical tests are performed.

HER and OER test. The HER and OER performance were tested in N_2 and O_2-saturated 0.1 M $HClO_4$. Before every test, the catalyst modified GCE was activating by cycling at -0.2-1.1 V (vs RHE) at 500 mV s^{-1} for 100 cycles. The polarization curves were conducted at a scan rate of 5 mV s^{-1} with 95 % iR drop compensation. The durability test was performed in 0.1 M $HClO_4$ solution using chronoamperometry. In addition, the LSV after 5000 cycles of CV was measured to further evaluate the stability of the catalyst. Electrochemical impedance spectroscopy (EIS) measurement was performed at a frequency of 0.1 Hz to 100 kHz in a 0.1 M $HClO_4$ solution.

Overall water splitting test. The overall water splitting tests were performed in a two-electrode system at

0.1 M $HClO_4$. Firstly, in three-electrode system, the prepared catalyst ink with a mass of 20 μg cm^{-2} was loaded on a 1 × 1 cm carbon fiber paper (CFP). Before every test, the surfaces of the prepared catalysts were cleaned by cyclic voltammetry between 1.0-1.6 V (vs RHE) at 500 mV s^{-1} for 100 cycles. Durability testing of overall water splitting was performed in two ways. On the one hand, chronoamperometry was performed at constant potential for 12 h to observe the change of current density (catalyst loading was 20 μg cm^{-2}); in addition, only the Pt-RuO_2@KB catalyst was chronoamperometric at constant potential for 150 h (catalyst loading was 100 μg cm^{-2}). On the other hand, chronopotentiometry experiments were performed at 10 mA cm^{-2} current density for 150 h (catalyst loading was 100 μg cm^{-2}).

Active sites calculations. The underpotential deposition (UPD) of copper (Cu) was used to calculate the active sites of the Pt-RuO_2@KB and other comparative samples. In this method, the number of active sites (n) can be calculated based on the UPD copper stripping charge (Q_{Cu}, $Cu_{upd} \rightarrow Cu^{2+}+2e^-$) using the following equation: $n = Q_{Cu} / (2 \times F)$, where F is the Faraday constant (96,485.3 C mol^{-1}).

ECSA measurements. The ECSA of the catalyst has been already proved could be calculated by Cu underpotential deposition (UPD) method. The ECSAs of catalysts were calculated by integrating the charge associated with oxidation of Cu (on the surface of catalyst by Cu-UPD) in electrolyte containing 50 mM $CuSO_4$ and 0.5 M H_2SO_4, by assuming a charge of 420 μC cm^{-2}. The ECSA can be calibrated as:

$$ECSA\ (cm^{-2}_{metal} / g_{metal}) = Q_{Cu} / (M_{metal} \times 420\ \mu C\ cm^{-2})$$

where M_{metal} is the mass loading of metal on a certain geometric area of the working electrode.

Measurement of the turnover frequency (TOF). The TOF (s^{-1}) was calculated by the following formula: TOF (s^{-1}) = I / (2 × F × n) (HER); TOF(s^{-1}) = I / (4 × F × n) (OER); where I is the current (A) during linear sweep voltammetry (LSV), F is the Faraday constant (96,485.3 C mol^{-1}), n is the number of active sites (mol). The factor 1/2 is based on the assumption that two electrons are necessary to form on hydrogen molecules. And the factor 1/4 is based on the assumption that two electrons are necessary to form on oxygen molecules. To obtain monolayer of copper, Pt-RuO_2@KB was first polarized at 0.25 V for 100 s. For the given polarization potential, there were only two oxidation peaks related to bulk and monolayer of Cu.

Calculation Setup. To investigate the electrocatalytic mechanism of the Pt-RuO_2 heterostructure, the slabs of Pt, RuO_2, and Pt-RuO_2 were established, respectively. DFT calculations of these slabs were computed by using a generalized gradient approximation (GGA) of exchange-correlation functional in the Perdew, Burke, and Ernzerhof (PBE). A plane-wave energy cut off of 400 eV was used together with norm-conserving pseudopotentials, and the Brillouin zone was sampled with a 2 × 2 × 1 Monkhorst–Pack grid. The structure was fully optimized until the force on each atom is less than 10^{-3} eV/Å. To avoid periodic interaction, a vacuum layer of 30 Å was incorporated into the slabs. The free energy (ΔG) was computed from $\Delta G = \Delta E + ZPE - T\Delta S$, where ΔE was the total energy, *ZPE* was the zero-point energy, the entropy (ΔS) of each adsorbed state were yielded from DFT calculation, and ΔU was applied potential, whereas the thermodynamic corrections for gas molecules were from standard tables.

Figures

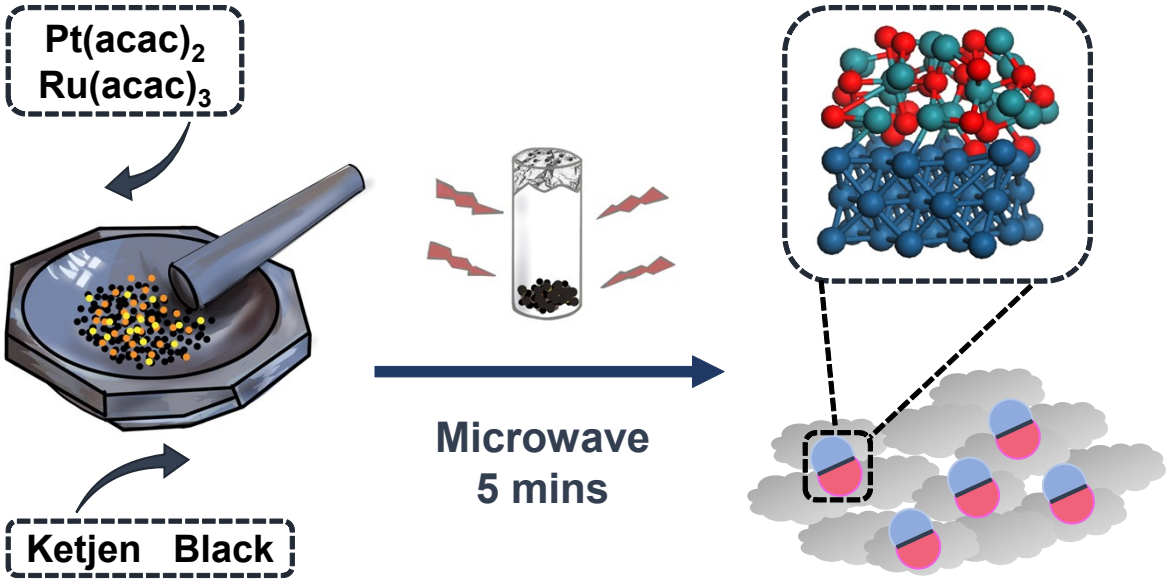

Figure S1. Schematic depiction of the synthesis of Pt-RuO_2@KB catalyst.

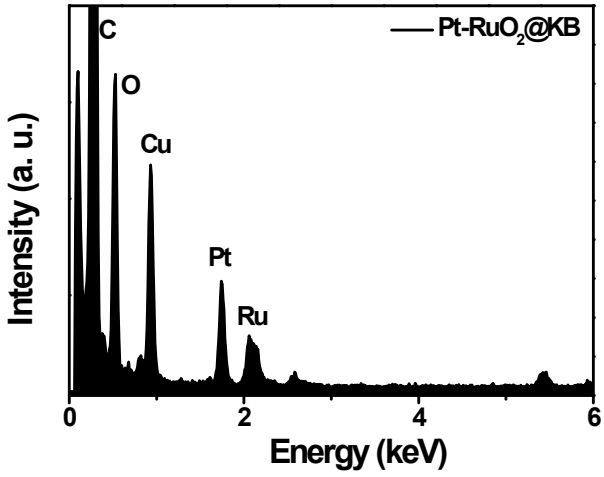

Figure S2. EDX spectrum of Pt-RuO_2@KB.

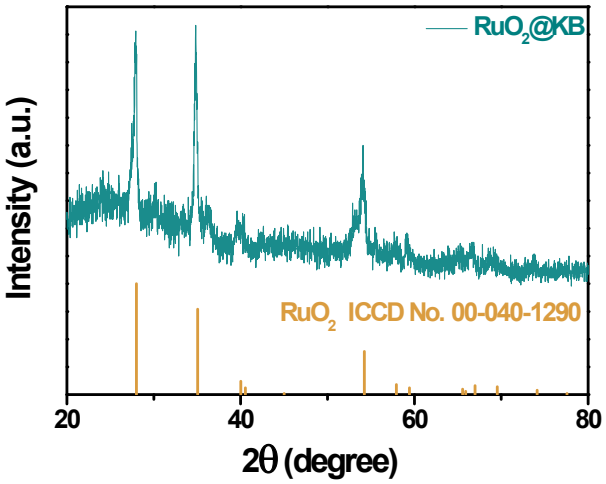

Figure S3. The XRD pattern of RuO_2@KB.

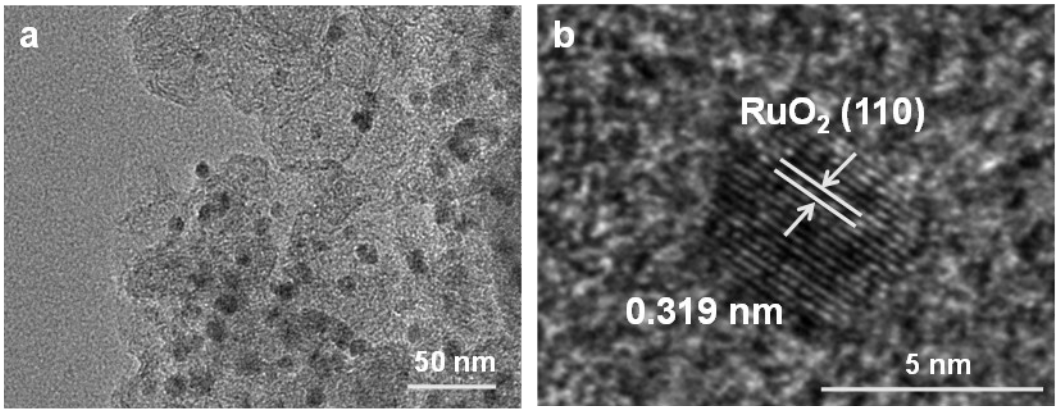

Figure S4. (a) TEM and (b) HRTEM images of RuO_2@KB.

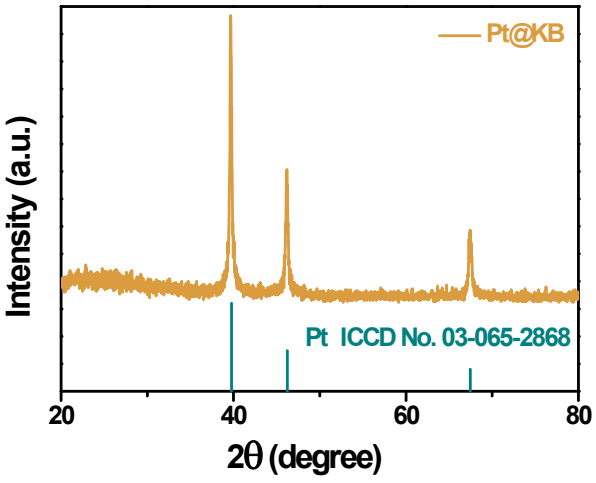

Figure S5. The XRD pattern of Pt@KB.

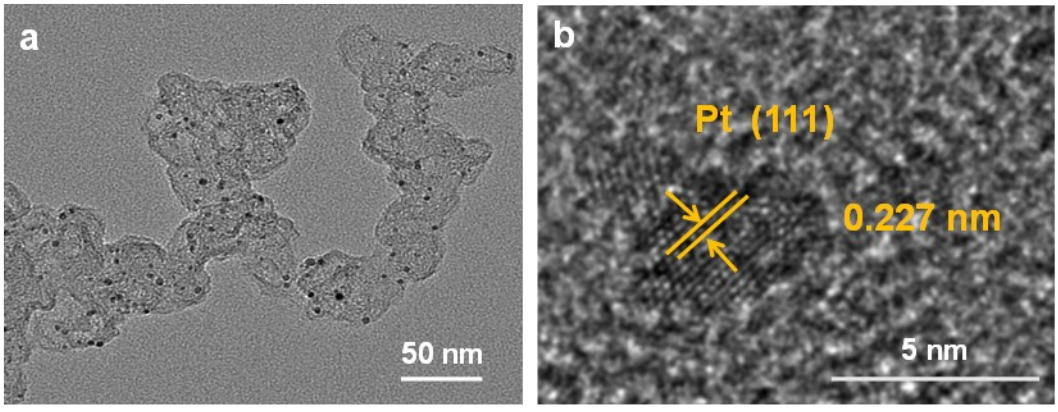

Figure S6. (a) TEM and (b) HRTEM images of Pt@KB.

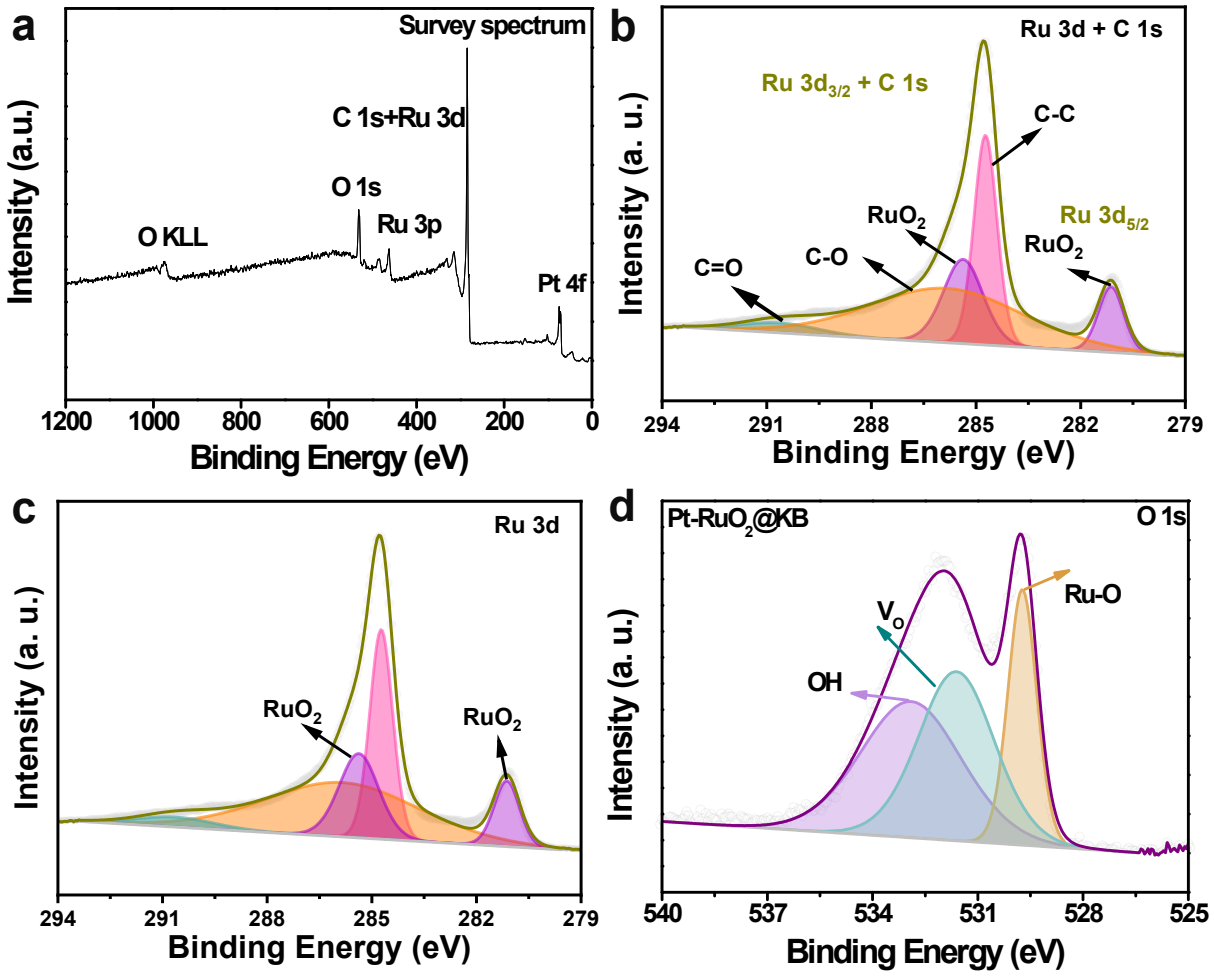

Figure S7. XPS spectra of Pt-RuO_2@KB. (a) Survey. (b) Ru 3d + C 1s. (c) Ru 3d. (d) O 1s.

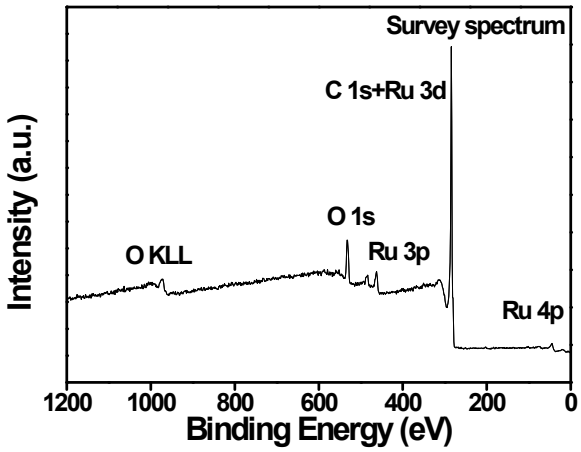

Figure S8. The survey XPS spectrum of the RuO_2@KB.

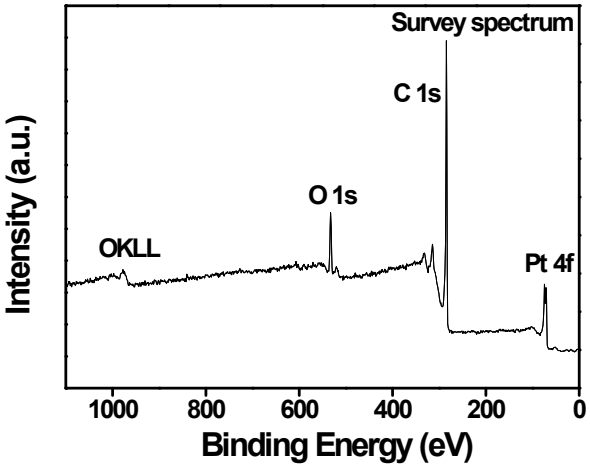

Figure S9. The survey XPS spectrum of the Pt@KB.

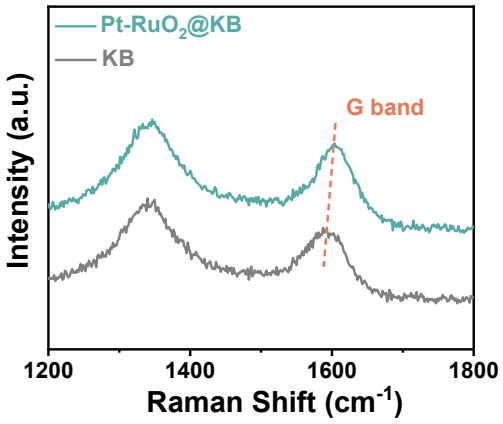

Figure S10. Raman spectra of Pt-RuO_2@KB and KB.

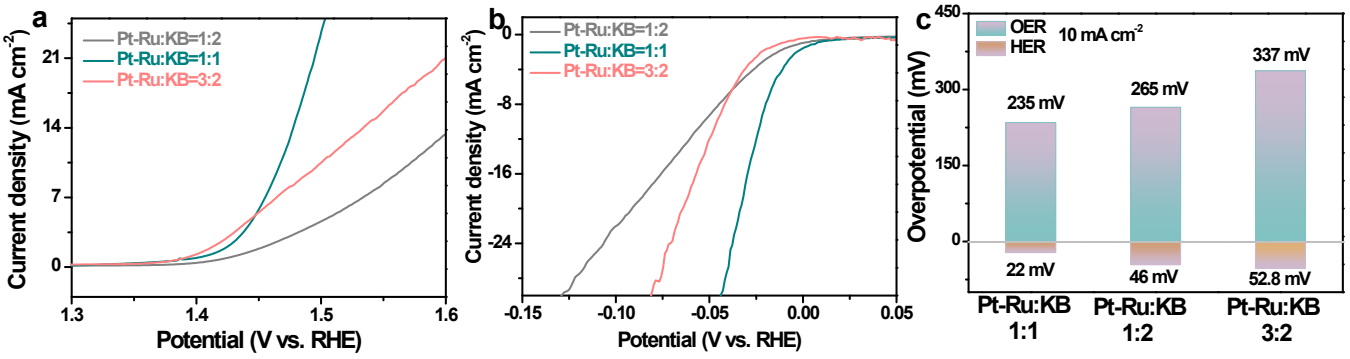

Figure S11. Pt-RuO_2@KB catalysts prepared at different Pt-Ru: KB ratios (1:2, 1:1, 3:2) in 0.1 M $HClO_4$ solution. (a) OER polarization curves. (b) HER polarization curves. (c) Comparison of overpotential changes at 10 mA cm^{-2}.

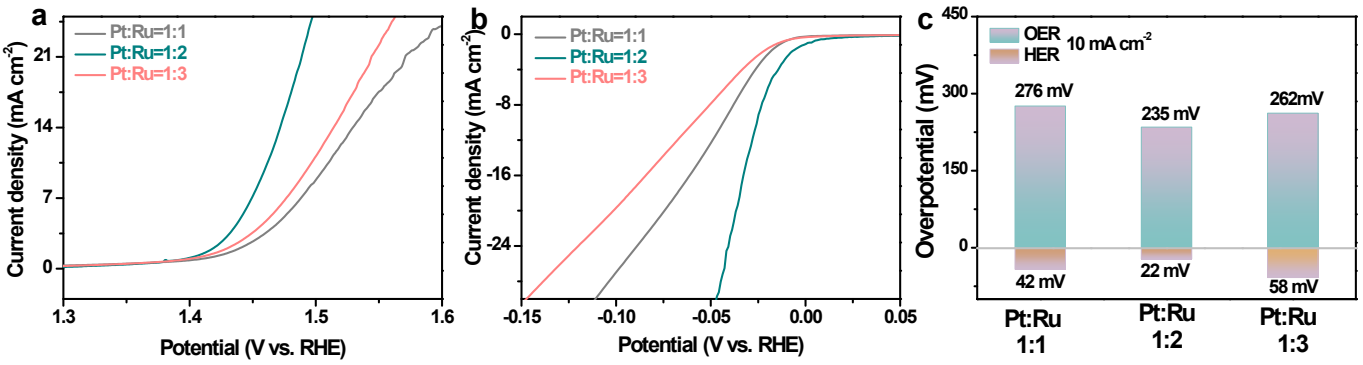

Figure S12. Pt-RuO_2@KB catalyst prepared at different Pt: Ru feed ratios of 1:1, 1:2 and 1:3 in 0.1 M $HClO_4$ solution. (a) OER polarization curves. (b) HER polarization curves. (c) Comparison of overpotential changes at 10 mA cm^{-2}.

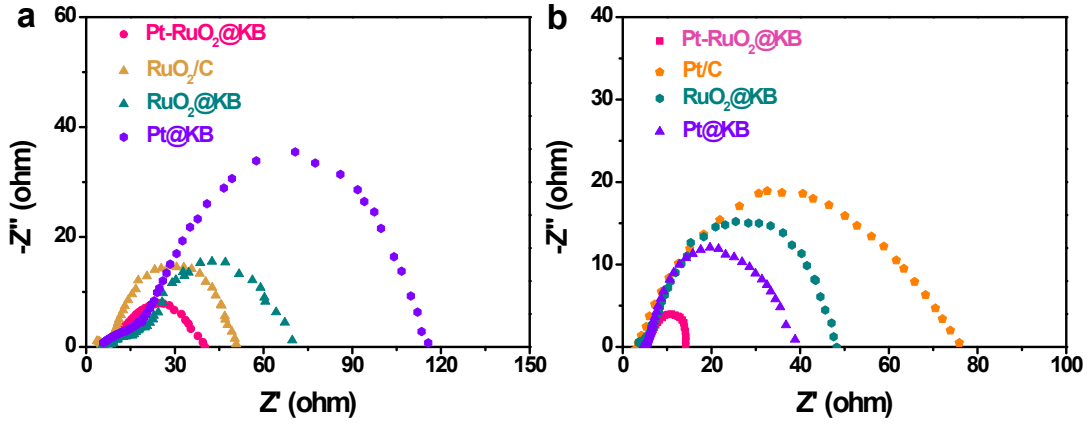

Figure S13. EIS Nyquist plots of Pt-RuO_2@KB, Pt@KB and RuO_2@KB catalysts. (a) OER. (a) HER.

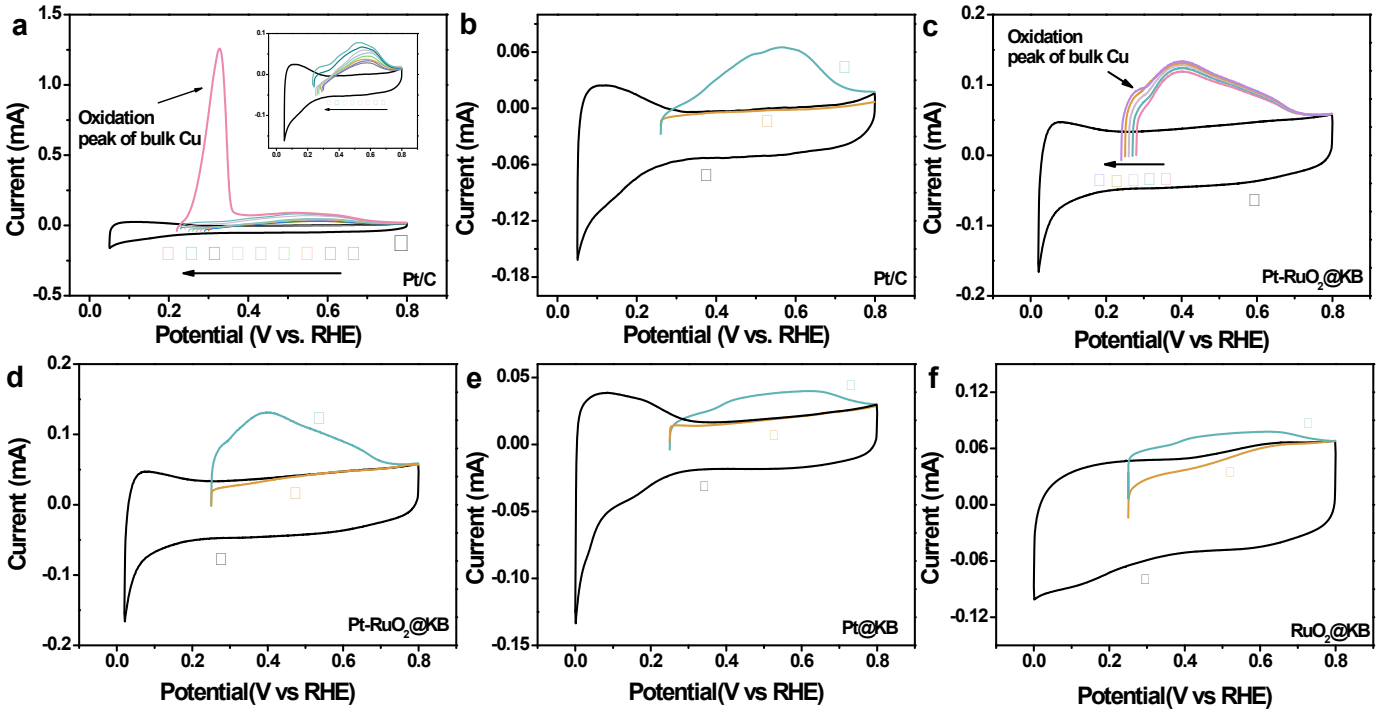

Figure S14. (a) Copper UPD in 0.5 M H_2SO_4 in the (I) absence and (II-X) presence of 5 mM $CuSO_4$ on Pt/C. For II-X, the electrode was polarized at 0.3 V, 0.29 V, 0.28 V, 0.27 V, 0.26 V, 0.25 V, 0.24 V, 0.23 V and 0.22 V for 100 s to form the UPD layers, respectively. (b) Copper UPD in 0.5 M H_2SO_4 in the (I, II) absence and (III) presence of 5 mM $CuSO_4$ on Pt/C. For II and III, the electrode was polarized at 0.26 V for 100 s to form the UPD layer. (c) Copper UPD in 0.5 M H_2SO_4 in the (I) absence and (II-VI) presence of 5 mM $CuSO_4$ on Pt-RuO_2@KB. For II-VI, the electrode was polarized at 0.28 V, 0.27 V, 0.26 V, 0.25 V and 0.24 V for 100 s to form the UPD layers, respectively. Copper UPD in 0.5 M H_2SO_4 in the absence and presence of 5 mM $CuSO_4$ on Pt-RuO_2@KB. The electrode was polarized at 0.25 V for 100 s to form the UPD layer. (d-f) Copper UPD in 0.5 M H_2SO_4 in the (I, II) absence and (III) presence of 5 mM $CuSO_4$ on Pt-RuO_2@KB, Pt@KB and RuO_2@KB, respectively. For II and III, the electrode was polarized at 0.25 V for 100 s to form the UPD layer.

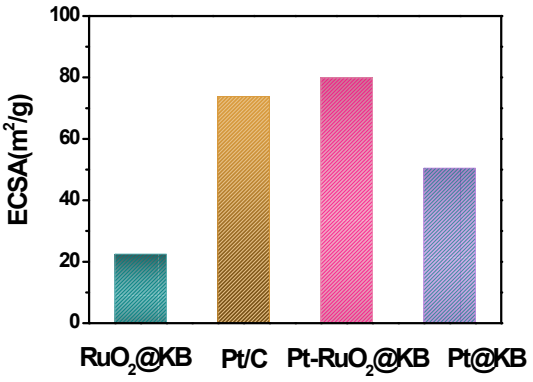

Figure S15. Estimation of the ECSA of RuO_2@KB, Pt/C, Pt-RuO_2@KB and Pt@KB, respectively.

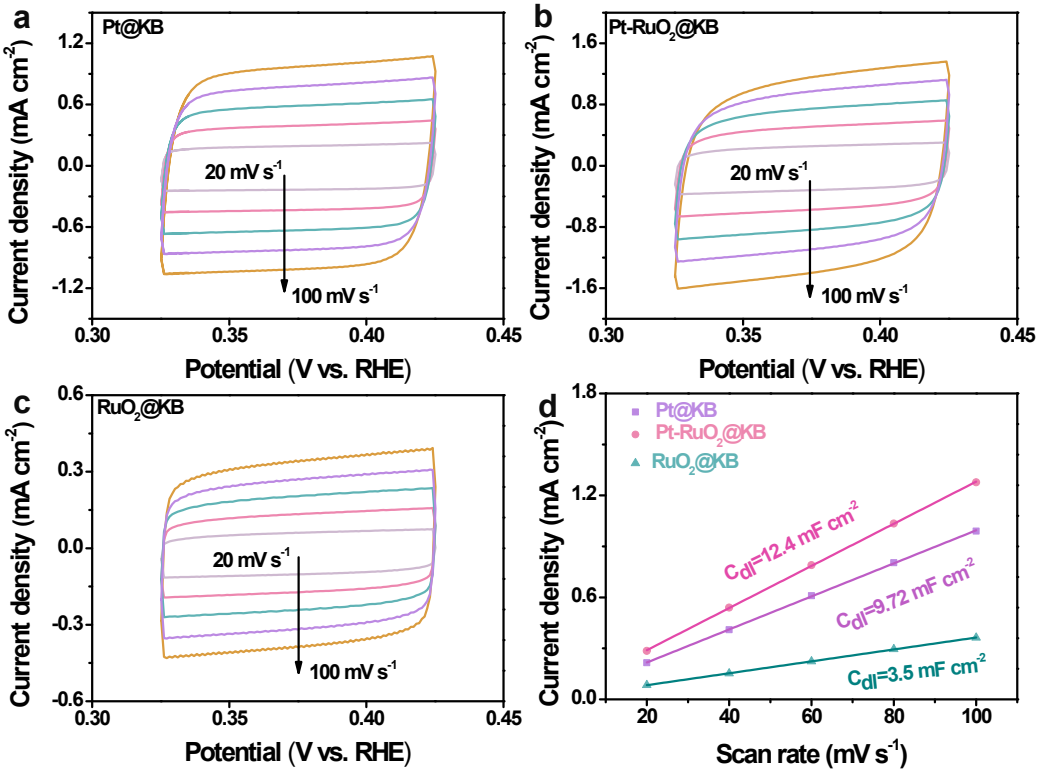

Figure S16. CV curves measured at different scan rates from 20 to 100 mV s^{-1} in 0.1 M $HClO_4$ for (a) Pt@KB, (b) Pt-RuO_2@KB and (c) RuO_2@KB. (d) Capacitive current at middle potential of CV curves as function of scan rates for Pt@KB, Pt-RuO_2@KB and RuO_2@KB.

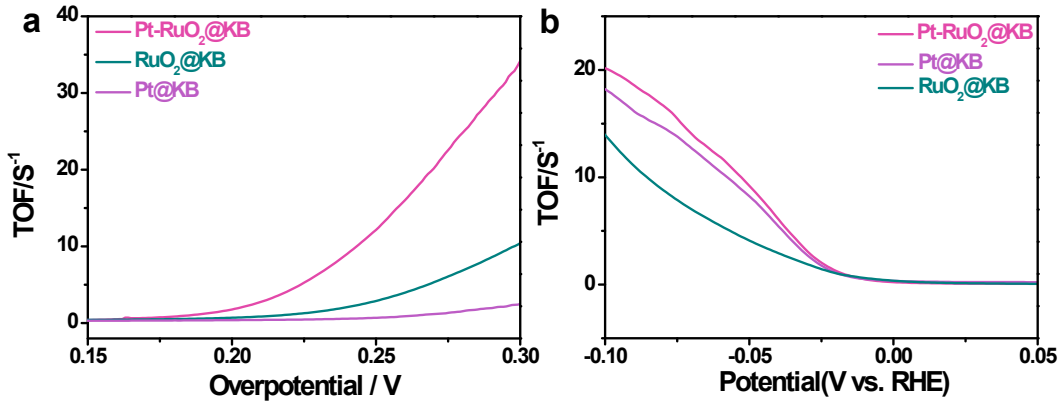

Figure S17. The potential-dependent TOF curves of Pt-RuO_2@KB, Pt@KB and RuO_2@KB catalysts. (a) OER. (b) HER.

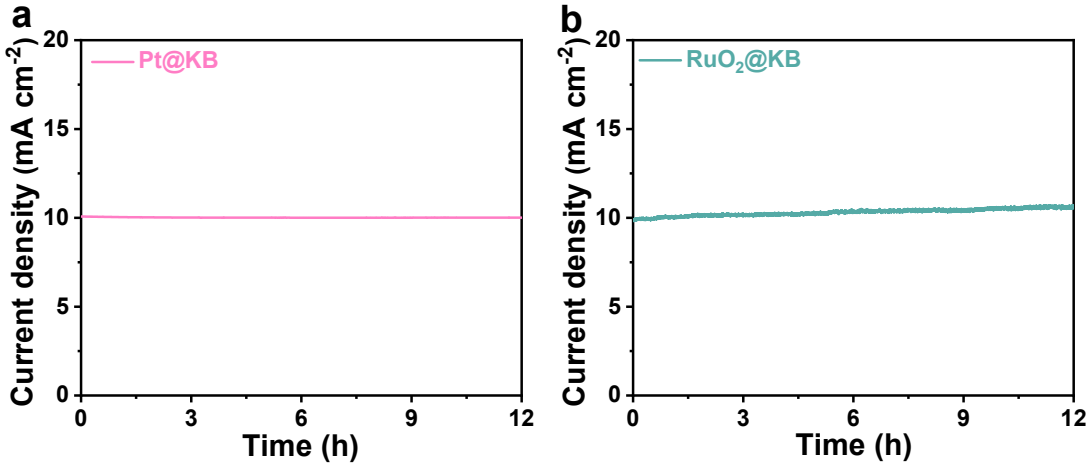

Figure S18. Current-time (i-t) stability curves up to 12 h duration of (a) Pt@KB, and (b)RuO_2@KB for OER.

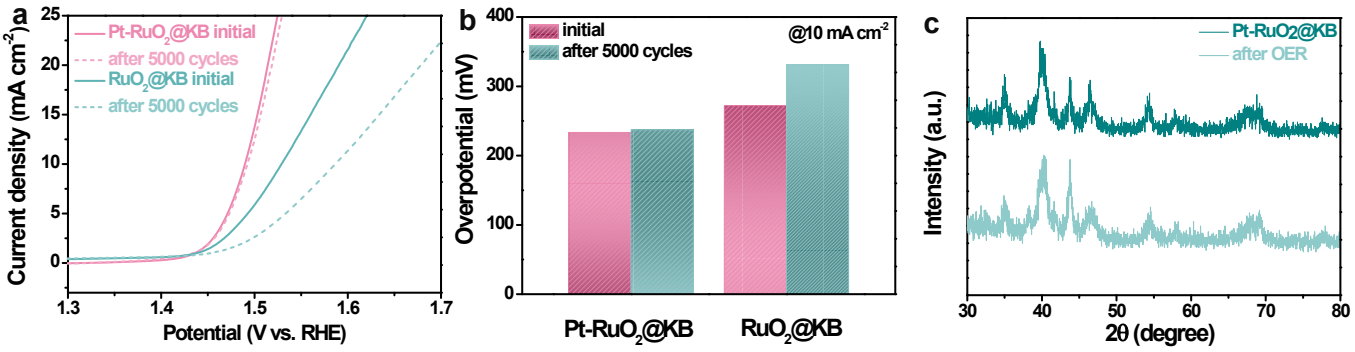

Figure S19. Electrocatalytic OER performance test of catalysts in 0.1 M $HClO_4$ solution. (a) Polarization curves for Pt-RuO_2@KB and RuO_2@KB before and after 5000 cycles. (b) Comparison of overpotential changes at 10 mA cm^{-2} and exchange current density. (c) Comparison of XRD for Pt-RuO_2@KB before and after reaction.

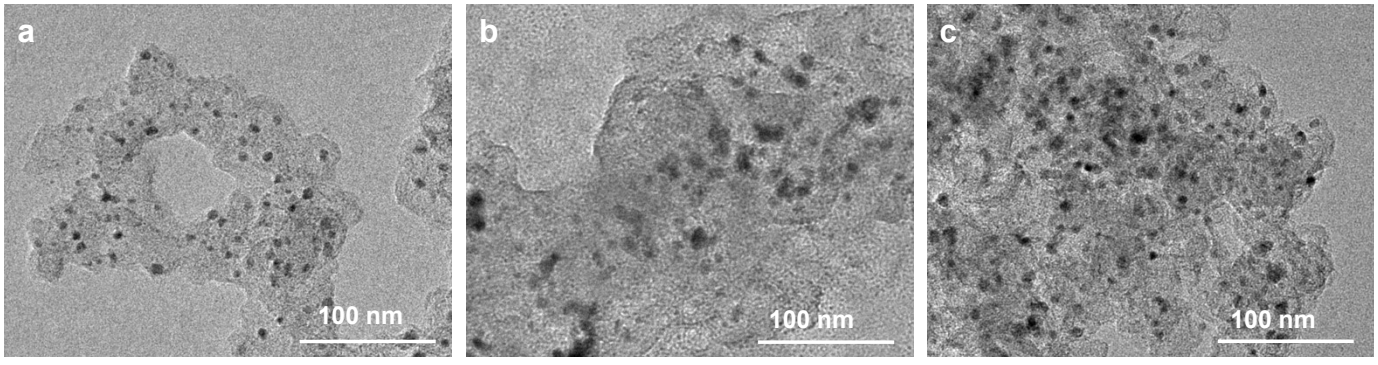

Figure S20. TEM images of (a) Pt-RuO_2@KB, (b) RuO_2@KB and (c) Pt@KB after OER, respectively.

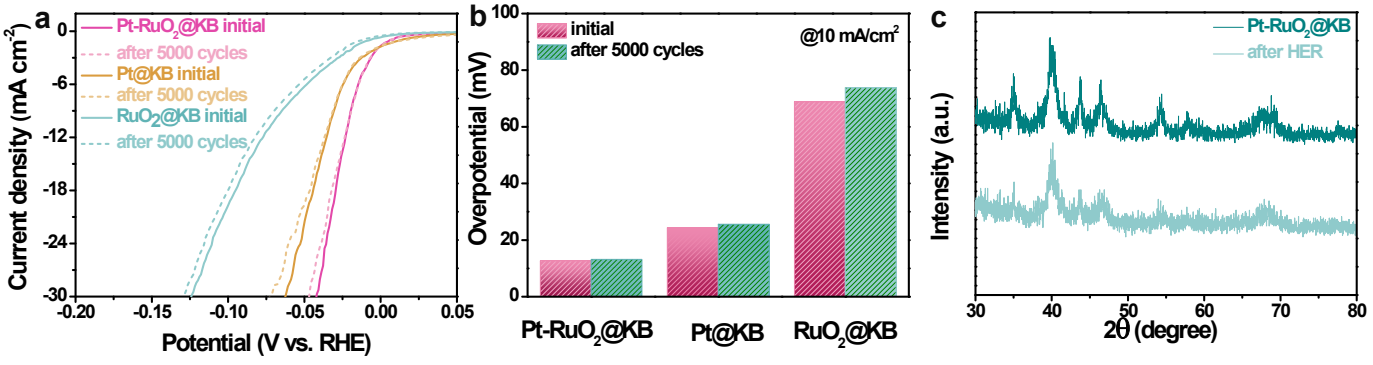

Figure S21. Electrocatalytic HER performance test of catalysts in N_2-saturated 0.1 M $HClO_4$ solution. (a) Polarization curves for Pt-RuO_2@KB, Pt@KB and RuO_2@KB before and after 5000 cycles. (b) Comparison of overpotential changes at 10 mA cm^{-2} and exchange current density. (c) Comparison of XRD for Pt-RuO_2@KB before and after reaction.

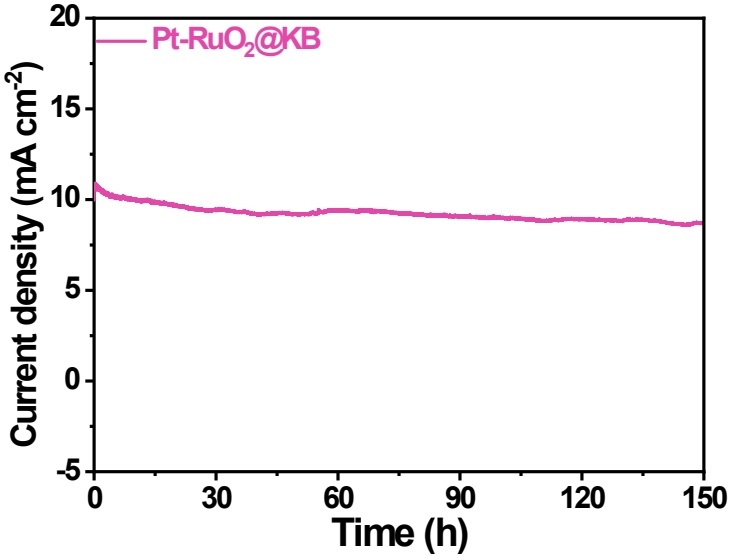

Figure S22. Chronoamperometry test at the applied potential of 1.54 V for 150 h of Pt-RuO_2@KB for overall water splitting in 0.1 M $HClO_4$.

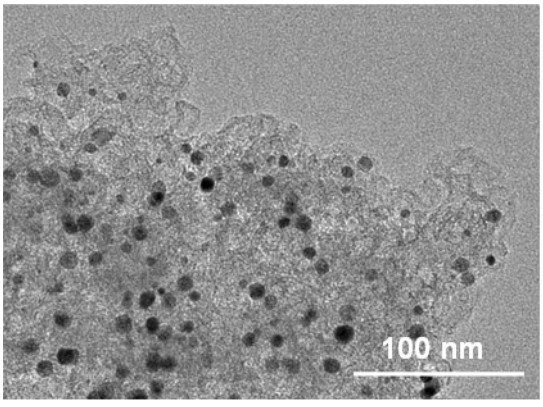

Figure S23. TEM image of Pt-RuO_2@KB after chronopotentiometry test for 150 h.

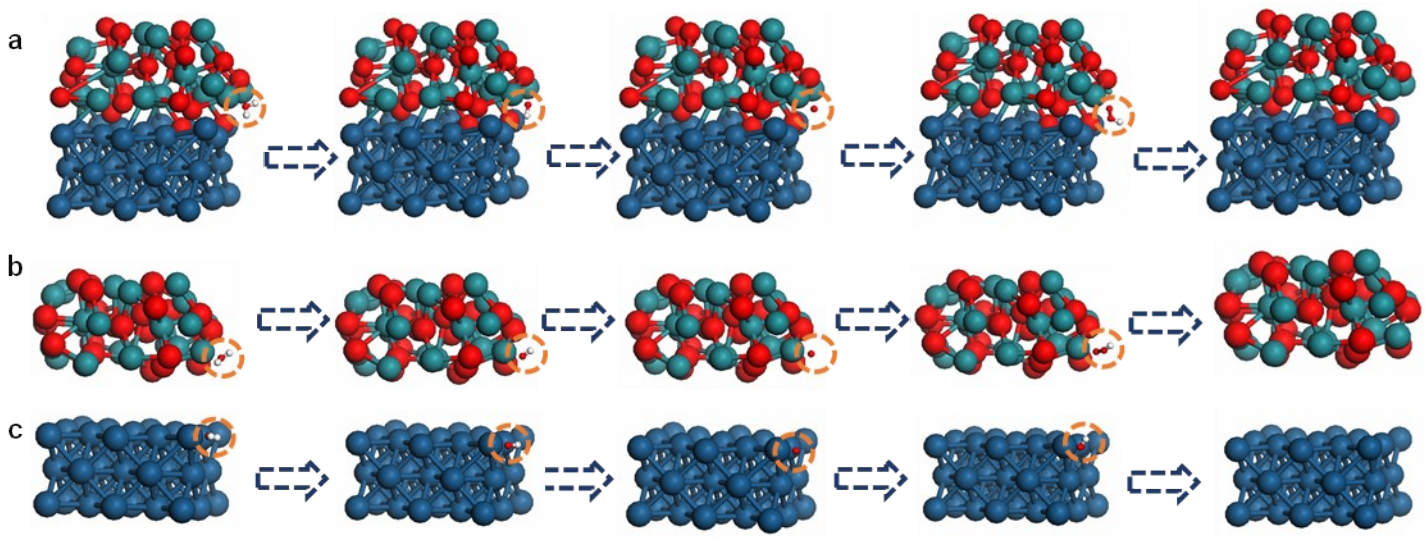

Figure S24. Reaction pathways of the OER occurring on the (a) Pt-RuO_2@KB, (b) RuO_2@KB and (c) Pt@KB. Blue, cyan, red, and white spheres represent Pt, Ru, O and H atoms, respectively.

Table S1. Atomic ratios of Pt-RuO_2@KB characterized by ICP.

Sample	Ru atom%	Pt atom%
Pt-RuO_2@KB	32	68

Table S2. The TOF of several catalysts at different overpotentials.

Sample	TOF (H_2 s^{-1}) @ Overpotential (mV)	TOF (O_2 s^{-1}) @ Overpotential (mV)	Reference
Pt-RuO_2@KB	**20.2 @ 100**	**34.5 @ 300**	**This work**
Pt@KB	**18.12 @ 100**	**2.5 @ 300**	**This work**
RuO_2@KB	**13.9 @ 100**	**10.5 @ 300**	**This work**
Pt-RuO_2@KB	**9.20 @ 50**	**12.2 @ 250**	**This work**
HP-Ru/C	2.04 @ 50	-	*Appl. Catal. B: Environ. 2021, 294, 120230*
Ru-RuO_2/CNT	0.12 @ 25	0.14 @ 250	*Nano Energy 2019, 61, 576*
Ru@C_2N	1.95 @ 50	-	*Nat. Nanotechnol. 2017, 12, 441*
Pt–V_2CT_x	4.76 @ 100	-	*Appl. Catal. B: Environ. 2022, 304, 120989*
IrNiCo PHNCs	-	0.26 @ 300	*Adv. Mater. 2017, 29, 1703798*
IrO x-Ir	-	10.6 @ 300	*Angew. Chem. Int. Ed. 2016, 55, 742*

Table S3. Comparison of HER activity for different electrocatalysts in acidic electrolytes.

Catalysts	Electrolyte	Overpotential (mV) @10 mA cm^{-2}	Tafel slope ($mV\ dec^{-1}$)	Reference
Pt-RuO_2@KB	**0.1 M $HClO_4$**	**22**	**24.3**	**This work**
IrTe NTs	0.5 M H_2SO_4	36	37.3	*J. Mater. Chem. A 2021, 9, 18576*
HP-Ru/C	0.5 M H_2SO_4	25	30.0	*Appl. Catal. B: Environ. 2021, 294, 120230*
Ru-RuO_2/CNT	0.5 M H_2SO_4	63	46	*Nano Energy 2019, 61, 576*
Rh-MoS_2	0.5 M H_2SO_4	47	24.0	*Adv. Funct. Mater. 2017, 27, 1700359*
IrCoNi-PHNC	0.1 M $HClO_4$	33	31.9	*Adv. Mater. 2017, 29, 1703798*
Ru@C_2N	0.5 M H_2SO_4	25	30.0	*Nat. Nanotechnol. 2017, 12, 441*
h-RuNPS	0.5 M H_2SO_4	29	33.0	*ACS Appl. Nano Mater. 2021, 4, 8530*
Mo_2C@NC@Pt	0.5 M H_2SO_4	27	28	*ACS Appl. Mater. Interfaces 2019, 11, 4047*
Pt-V_2CT_x	0.5 M H_2SO_4	27	36.5	*Appl. Catal. B: Environ. 2022, 304, 120989*
PtN_x/TiO_2	0.5 M H_2SO_4	67	34	*Nano Energy 2020, 73, 104739*
$PdSn_4$	0.5 M H_2SO_4	50	83	*ACS Catal. 2021, 11, 7311-7318*
IrO_2/V_2O_5	0.5 M H_2SO_4	266	56	*Adv. Sci. 2022, 9, 2104636*
Pt_{SA}-Ni_3S_2	0.5 M H_2SO_4	33	34.7	*Adv. Sci. 2021, 8, 2100347*
Pt-C_3	0.5 M H_2SO_4	30	53	*J. Am. Chem. Soc. 2022, 144, 2171−2178*
F-SnO_2@Pt	0.5 M H_2SO_4	42	34	*ACS Nano 2022, 16, 1625−1638*

Table S4. Comparison of OER activity for different electrocatalysts in acidic electrolytes.

Catalysts	Electrolyte	Overpotential (mV) @10 mA cm^{-2}	Tafel slope (mV dec^{-1})	Reference
Pt-RuO_2@KB	**0.1 M $HClO_4$**	**235**	**61.9**	***This work***
H-Ti@IrOx	0.5 M H_2SO_4	277	29	*J. Mater. Chem. A. 2020, 8, 24743*
IrCo hollow nanosphere	0.5 M H_2SO_4	284	66.7	*Nanoscal. 2020, 12, 24070*
RuO_2/Co_3O_4-RuCo@NC	0.5 M H_2SO_4	247	89	*ACS Appl. Mater. Interfaces 2019, 11, 47894*
RuCu NSs/C-350	0.5 M H_2SO_4	236	-	*Angew. Chem. Int. Ed. 2019, 58, 13983*
$NaRuO_2$	0.1 M $HClO_4$	255	38	*Adv. Energy Mater. 2019, 9, 1803795*
Co-RuIr	0.1 M $HClO_4$	235	-	*Adv. Mater. 2019, 31, 1900510*
$Y_{1.85}Zn_{0.15}Ru_2O_7$ -δ	0.5 M H_2SO_4	291	36.9	*Appl. Catal. B: Environ. 2019, 244, 494*
Ir WNWs	0.1 M $HClO_4$	280	47.8	*Nanoscale 2018, 10, 1892*
Ir/GF	0.5 M H_2SO_4	290	46	*Nano Energy 2017, 40, 27*
IrNiCo PHNCs	0.1 M $HClO_4$	303	53.8	*Adv. Mater. 2017, 29, 1703798*
IrOx-Ir	0.5 M H_2SO_4	290	44.7	*Angew. Chem. Int. Ed. 2016, 55, 742*
IrOx/Graphdiyne	0.5 M H_2SO_4	236	70	*Adv. Energy Mater. 2021, 11, 2101138*
RuO_2-WC NPs	0.5 M H_2SO_4	347	88.5	*Angew. Chem. Int. Ed. 2022, 16, 202202519*
IrO_2/V_2O_5	0.5 M H_2SO_4	266	56	*Adv. Sci. 2022, 9, 2104636*
Ru@Ir–O	0.5 M H_2SO_4	238	91.3	*Small 2022, 18, 2108031*
IrO_2/$LiLa_2IrO_6$	0.1 M $HClO_4$	278	45	*J. Mater. Chem. A, 2022, 10, 3393 – 3399*

Table S5. Performance comparison of Pt-RuO_2@KB and some recently reported representative catalyst pairs for overall water splitting in different electrolytes.

Catalysts	Electrolyte	Overall voltage (V) @10 mA cm^{-2}	Reference
Pt-RuO_2@KB	**0.1 M $HClO_4$**	**1.54**	***This work***
Ir-NR/C (+, -)	0.5 M H_2SO_4	1.55	*Appl. Catal. B: Environ. 2020, 279, 119394*
Co_3O_4-RuCo@NC	0.5 M H_2SO_4	1.66	*ACS Appl. Mater. Interfaces 2019, 11, 47894*
IrW nanobranches	0.5 M H_2SO_4	1.58	*Nanoscal. 2019, 11, 8898*
IrNi NCs	0.5 M H_2SO_4	1.58	*Adv. Funct. Mater. 2017, 27, 1700876*
Co-RuIr	0.1 M $HClO_4$	1.52	*Adv. Mater. 2019, 31, 1900510*
a-$RuTe_2$ PNRs	0.5 M H_2SO_4	1.52	*Nat. Commun. 2019, 10, 5692*
Ru/RuS_2 heterostructure	0.5 M H_2SO_4	1.501	*Angew. Chem. Int. Ed. 2021, 60, 12328*
IrTe NTs	0.5 M H_2SO_4	1.53	*J. Mater. Chem. A 2021, 9, 1857*

Table S6. Comparison of the long-term stability of bifunctional electrocatalysts for overall water splitting in acidic environments.

Catalysts	Electrolyte	overall water splitting work life	Reference
Pt-RuO_2@KB/CFP	**0.1 M $HClO_4$**	**150 hr**	***This work***
RuO_2/Co_3O_4− RuCo@NC	0.5 M H_2SO_4	8 hr	*ACS Appl. Mater. Interfaces 2019, 11, 47894*
Co-RuIr	0.1 M $HClO_4$	25 hr	*Adv. Mater. 2019, 31, 1900510*
IrW	0.1 M $HClO_4$	8 hr	*ACS Central. Sci. 2018, 4, 1244*
IrCoNi	0.1 M $HClO_4$	1000 cycles	*Adv. Mater. 2017, 29, 1703798*
Ir/GF	0.5 M H_2SO_4	10 hr	*Nano Energy 2017, 40, 27*
single-site Pt-doped RuO_2 hollow nanospheres	0.5 M H_2SO_4	100hr	*Sci. Adv.2022, 8, eabl9271*
Ir NW	0.1 M $HClO_4$	11.1 hr	*Nanoscale 2018, 10, 1892*
Ir NP	0.5 M $HClO_4$	5.6 hr	*Chem. Front. 2018, 5, 1121*